LA-UR-08-5929

Approved for public release; distribution is unlimited.

Title:	"Recent High-Magnetic-Field Experiments on the "High Tc" Cuprates; Fermi-Surface Instabilities as a Driver for Superconductivity"
Author(s):	John Singleton, Ross McDonald, & Susan Cox MPA-NHMFL/LANL
Intended for:	Proceedings of the Journal of Physica B ECRYS Conference (ECRYS-2008) 5th International Workshop on Electronic Crystals August 24-30, 2008

Form 836 (7/06)

Recent high-magnetic-field experiments on the "High T_c" cuprates; Fermi-surface instabilities as a driver for superconductivity

John Singleton Ross D. McDonald and Susan Cox

National High Magnetic Field Laboratory, TA-35, MS-E536, Los Alamos National Laboratory, Los Alamos, New Mexico 87545, USA

Abstract

We give a brief review of high-magnetic-field quantum-oscillation measurements on cuprate superconductors. In the case of the underdoped cuprates, a number of small Fermi-surface pockets are observed, probably due to the incommensurate nesting of the predicted (large) hole Fermi surface. The Fermi-surface instabilities that drive this nesting are also likely to result in the the incommensurate spin fluctuations observed in inelastic neutron-scattering measurements. We suggest that the unusually high superconducting transitions in the cuprates are driven by an exact mapping of these incommensurate spin fluctuations onto the $d_{x^2-y^2}$ Cooper-pair wavefunction. The maximum energy of the fluctuations $\sim$ 100s of Kelvin gives an appropriate energy scale for the superconducting transition temperature.

Recent improvements in pulsed-magnetic-field techniques have permitted the observation of magnetic quantum oscillations in the "High T_c" cuprate superconductors [1–7]. Figure 1 shows some typical data, in this case for $YBa_2Cu_3O_{6.60}$ [5]. The experiment uses the MHz penetration technique reported in Ref. [2] in which a small single crystal is placed within the coil of a tank circuit; changes in sample resistivity alter the coil inductance, which in turn shift the tank circuit's resonant frequency. The superconducting to normal transition is seen as a sharp fall in frequency at around 28 T; at higher fields, Shubnikov-de Haas oscillations are visible in the raw data. Suitable background subtraction [2,4] reveals two series of oscillations with frequencies 590 ± 20 T and 1990 ± 40 T [5].

The data shown in Fig. 1 are typical of the underdoped cuprates, for which several studies suggest a number (1-3) of small Fermi-surface pockets (quantum-oscillation frequencies $\lesssim$ 2000 T) [1–9]; a summary is given in Table 1. Such pockets are likely to result from the incommensurate nesting of the predicted (large) hole Fermi surface [2,4,6,7]; the nesting vectors inferred [4] are consistent with the wavevectors of the spin fluctuations determined in the neutron-scattering measurements [10–15] . This strongly suggests that the fluctuations are driven by Fermi-surface instabilities [4], and that the development of their dispersion with increasing hole doping p [10–15] reflects the evolution of the underlying Fermi-surface topology.

The fact that the Fermi-surface reconstruction [4] seems to be intimately related to the antiferromagnetic spin fluctuations seen in neutron scattering [10–15] naturally leads one to ask whether the same mechanism is involved in cuprate superconductivity [16]. Low-energy inelastic neutron-scattering data for both $La_{2-x}Sr_xCuO_4$ [12,15] and $YBa_2Cu_3O_{7-x}$ [13,14] follow an approximately inverted parabolic form

$$E(\mathbf{q}) = E_0 \left(1 - \frac{a^2(\mathbf{q}-\mathbf{Q}_0)^2}{\pi^2\delta^2}\right), \qquad (1)$$

where a is the in-plane lattice parameter and $E_0 \approx 30 - 40$ meV is a doping-dependent energy scale [10–14]. Here, δ depends on the composition and hole doping p of the cuprate involved [10,11,17]; some values are given in Table 2. As $E \to 0$, the brightest scattering intensity typically appears at a cluster of four incommensurate peaks at $\mathbf{Q} = (\pm\pi/a, \pm(1 \pm 2\delta)\pi/a)$ and $(\pm(1 \pm 2\delta)\pi/a, \pm\pi/a)$ [10–

Table 1
Parameters measured in cuprate quantum-oscillation experiments. In underdoped cuprates (first three rows), frequencies < 2000 T are seen, corresponding to small Fermi-surface pockets. These are attributed [4] to an α electron pocket and β hole pocket, thereby accounting for the electronic heat capacity. In addition, a frequency $\sim$ 200 T named γ may be present in the underdoped cuprates [4,8,9]. By contrast, overdoped $Tl_2Ba_2CuO_{6+\delta}$ shows a single high frequency [9] corresponding to the unreconstructed Fermi surface.

Compound	F_α (T)	m^*_α (m_e)	F_β (T)	m^*_β (m_e)	Reference
$YBa_2Cu_3O_{6.51}$	520 ± 10	2.2 ± 0.1	1650 ± 40	3.8 ± 0.1	[1,4]
$YBa_2Cu_3O_{6.60}$	590 ± 20	2.7 ± 0.3	1990 ± 40	4.0 ± 0.5	[5]
$YBa_2Cu_4O_8$	670 ± 30	3.0 ± 0.3	undetected		[2,3]
$Tl_2Ba_2CuO_{6+\delta}$	18100 ± 50	4.1 ± 1			[9]

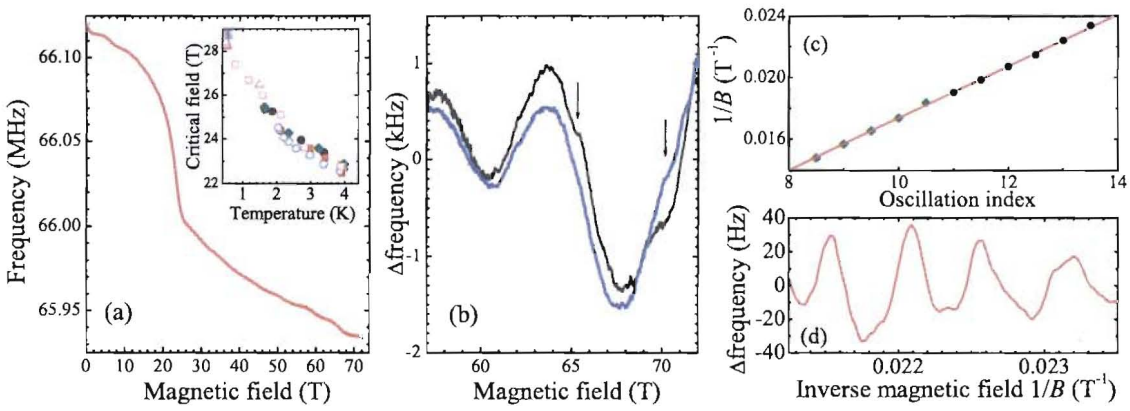

Fig. 1. (a) MHz penetration data from a single crystal of $YBa_2Cu_3O_{6.60}$ (T = 1.49 K) recorded in the 75 T short-pulse magnet at Los Alamos; the superconducting to normal transition is the sharp drop around 28 T. Inset: measured critical field versus temperature for the same crystal for many different dB/dt values in the range $\sim 250-25000$ Ts^{-1}, illustrating that inductive sample heating is minimal. (b) After the subtraction of a suitable background, Shubnikov-de Haas oscillations of frequency $F_\alpha = 590 \pm 20$ T are visible in the data; the arrows indicate a second set of oscillations of a higher frequency (see (d)). Sample temperatures are 1.49 K (black) and 2.08 K (blue). (c) Oscillation inverse-field positions versus index; data from the 60 T long-pulse (black) and 75 T short-pulse (green) magnets are shown. The straight line gives $F_\alpha = 590 \pm 20$ T. (d) Oscillations of frequency $F_\beta = 1990 \pm 40$ T visible in MHz data obtained in the 60 T long-pulse magnet. (After Ref. [5].)

15]. A simple model of spin fluctuations that can produce these peaks is a sinusoidal variation of the staggered moment modulated by an exponential damping factor [16]; the latter term represents the fact that the antiferromagnetic fluctuations possess a finite correlation length ξ [11,17]. The spatially-varying moment is thus

$$s(\mathbf{r},t) = \sum_{\mathbf{Q}} s_{\mathbf{Q}} \exp(-\frac{r}{\xi} + i\omega t)\cos(\mathbf{Q}.(\mathbf{r}-\mathbf{r}_0)), \qquad (2)$$

where ω is the angular frequency of the fluctuations, $\mathbf{r}_0 = (\pm d, 0)$ or $(0, \pm d)$ with $d = a/2\delta$, and the sum in $\mathbf{Q}$ runs over the values given above. In reproducing the general form of the experimental neutron data [10–15], the choice of $\mathbf{r}_0$ is quite critical; any other value would give significant intensity at $\mathbf{q} = \mathbf{Q}_0$, at variance with the experimental spectra.

The form of Eq. 2 is very similar to the two-dimensional $d_{x^2-y^2}$ Cooper-pair wavefunction in real space [18,19]:

$$\psi(\mathbf{r}) \propto \cos(rk_F)(x^2-y^2)e^{-3r/\xi_0}. \qquad (3)$$

Here $r = \sqrt{x^2+y^2}$ is the cylindrical polar radius, x and y are corresponding Cartesian coordinates, k_F is the Fermi wavevector [1,2] and ξ_0 is the superconducting coherence length, the lengthscale over which $\psi(\mathbf{r})$ is non-negligible. Coherence lengths ξ_0 derived from magnetoresistance and other data [20,21] are given in Table 2 for several cuprates with different composition and hole doping p.

The parameter d plays a similar role in the spin-fluctuation spatial distribution to that of ξ_0 in the Cooper-pair wavefunction: d determines the lengthscale over which the spin-fluctuation magnitude is largest. Values of $d = a/2\delta$ may be deduced using the δ taken from inelastic neutron-scattering measurements shown in Table 2. In the $La_{2-x}Ca_xCuO_4$ cuprates, the dispersion relationships have been measured down to low energies, providing accu-

Table 2
Parameters for various cuprate superconductors, including hole doping p. For $La_{2-x}Sr_xCuO_4$, δ values measured at neutron transfer energies of $E \approx$ 2-3 meV are taken from Refs. [12,15]. For $YBa_2Cu_3O_{7-x}$, δ values at the equivalent energy are taken from plots such as Fig. 2a using data from Refs. [13,14]. Correlation lengths ξ are taken from Ref. [11] while BCS coherence lengths ξ_0 are taken from Refs.[20,21], occasionally requiring interpolation between adjacent compositions for precise doping matches to δ.

Compound	p	δ	ξ (Å)	ξ_0 (Å)	T_c (K)
$La_{1.94}Sr_{0.06}CuO_4$	0.06	0.05	17	56	13
$La_{1.925}Sr_{0.075}CuO_4$	0.075	0.07	14	44	33
$La_{1.92}Sr_{0.08}CuO_4$	0.08	0.08	11	36	24
$YBa_2Cu_3O_{6.5}$	0.082	0.078	9	33	59
$YBa_2Cu_3O_{6.6}$	0.097	0.16	7.5	22	62.7
$La_{1.9}Sr_{0.1}CuO_4$	0.10	0.10	12	27	29
$YBa_2Cu_3O_{6.8}$	0.123	0.18	4	24	71.5
$La_{1.88}Sr_{0.12}CuO_4$	0.12	0.115	17	25	33.5
$La_{1.86}Sr_{0.14}CuO_4$	0.14	0.1225	12	22	35
$La_{1.85}Sr_{0.15}CuO_4$	0.15	0.1225	14	20	38
$YBa_2Cu_3O_{6.95}$	0.152	0.24	3.3	12	93
$La_{1.82}Sr_{0.18}CuO_4$	0.18	0.13	9	19	35.5
$La_{1.75}Sr_{0.25}CuO_4$	0.25	0.125	8	28	15
$La_{1.73}Sr_{0.27}CuO_4$	0.27	0.1	10	34	7

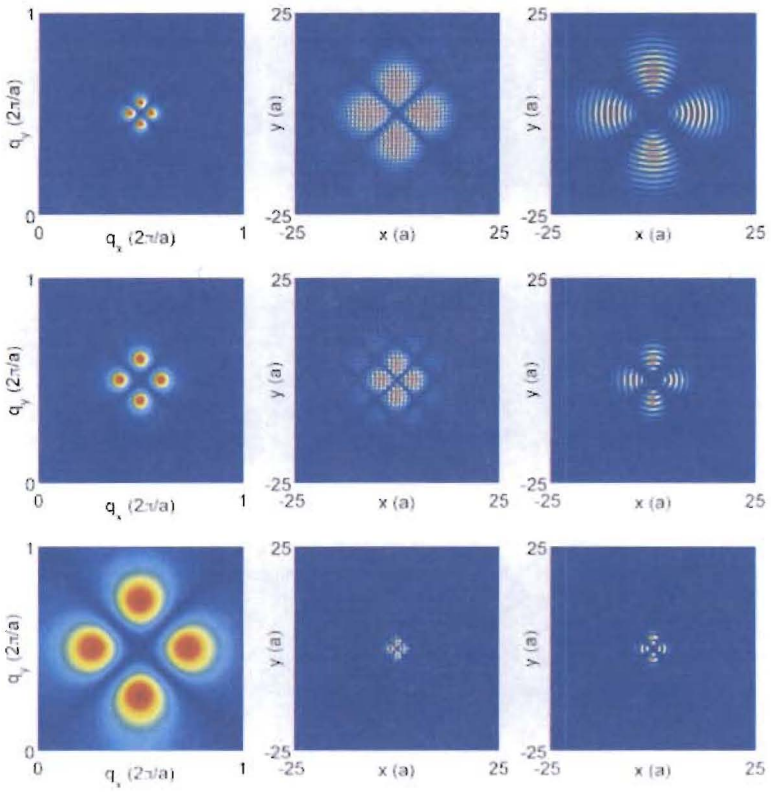

Fig. 2. Comparisons of the spin density amplitude and $d_{x^2-y^2}$ wavefunction at selected values of p [16]. The first column shows plots of the incommensurate diffraction peaks obtained on re-Fourier transforming $s(\mathbf{r})$ calculated using Eq. 2 and the published values of δ and ξ listed in Table 2. The second column shows the calculated $|s(\mathbf{r})|$ while the third column shows $\rho_c(\mathbf{r}) = |\Psi(\mathbf{r})|^2$ calculated according to the values of ξ_0 listed in Table 2. Rows 1, 2 and 3 consecutively correspond to $p \approx 0.06$, 0.1 and 0.152.

rate values of δ [12]. However, there is a loss of intensity at lower energy transfers in $YBa_2Cu_3O_{7-x}$, possibly because of their greater homogeneity [13,14], necessitating a downward extrapolation of the dispersion curves to obtain δ in the limit $E \to 0$.

Having tabulated experimental values of δ and ξ_0 for various hole densities p (Table 2), we can now plot the evolution with increasing p of the spatial distribution of the spin fluctuations (Eq. 2) alongside the corresponding Cooper-pair wavefunction (Eq. 3); Fig. 2 shows the result. At small values of p, the incommensurate neutron-scattering peaks occupy a small area of k-space [12–14]; the corresponding real-space spin-fluctuation distribution occupies a large area, as does the Cooper-pair wavefunction. As p increases, the incommensurate peaks spread out in k-space [12–14]; hence, the spin-fluctuation spatial distribution is compressed, as is the Cooper-pair wavefunction. Although the tabulated values of ξ_0 and δ (Table 2) are deduced from completely independent experiments (the former from thermodynamic or transport data, the latter from neutron scattering), there is a very close match between the physical size of the $d_{x^2-y^2}$ Cooper-pair wavefunction and the spatial extent of the spin-fluctuation distribution.

The very similar spatial extent of the Cooper-pair wavefunction and the spin fluctuations strongly suggests a

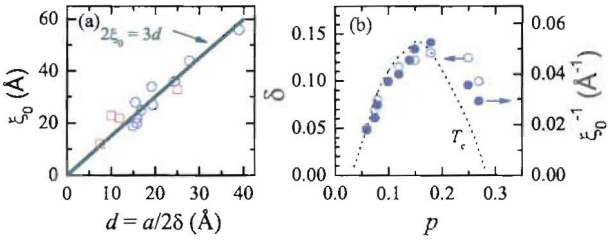

Fig. 3. (a) The approximately linear correspondence between $d = a/2\delta$ and ξ_0 for $La_{2-x}Sr_xCuO_4$ (circles) and $YBa_2Cu_3O_{7-x}$ (squares). The line represents the ratio $2\xi_0 = 3d$ (Eq. 4). (b) Plot showing δ and ξ_0^{-1} in $La_{2-x}Sr_xCuO_4$ exhibiting a maximum versus p in a similar fashion to T_c (scaled for comparison), though T_c falls more rapidly with p beyond optimal doping [16].

causal relationship between the two phenomena. Examination of Eqs. 3 and 2 shows that the spin fluctuation amplitude is largest at the vector locations $(\pm d, 0)$ and $(0, \pm d)$, whilst the $d_{x^2-y^2}$ Cooper-pair wavefunction has greatest probability amplitude at $(\pm\frac{2}{3}\xi_0, 0)$ and $(0, \pm\frac{2}{3}\xi_0)$. Therefore, if the spin fluctuations are responsible for the superconducting pairing, one would expect that

$$2\xi_0 = 3d, \tag{4}$$

independent of hole doping p. Fig. 3a, which plots experimental values of ξ_0 against d (from Table 2), shows that this is in fact the case for *both* $La_{2-x}Sr_xCuO_4$ *and*

$YBa_2Cu_3O_{7-x}$. Irrespective of doping and composition, the data for all materials lie close to the single straight line $2\xi_0 = 3d$ (Eq. 4). This suggests that the same causal connection between the spin fluctuations and superconductivity holds for *all* of the cuprates.

Further support for such an idea comes from the matching phase of the $d_{x^2-y^2}$ wavefunction and the spin fluctuations; on setting $\mathbf{r}_0 = (\pm d, 0)$ or $(0, \pm d)$ where $d = a/2\delta$, the π difference in phase between the adjacent 'spin clusters' (Fig. 2) is aligned with the π difference in phase between adjacent lobes of the $d_{x^2-y^2}$ Cooper-pair wavefunction (Fig. 2). The spin fluctuations are therefore "in phase" with the Cooper-pair wavefunction.

Incommensurate diffraction peaks in metallic systems are almost always associated with Fermi-surface nesting, in which the periodicity of spin or change modulation is determined by the topology of the Fermi surface [22]. In such a picture, the cuprate Fermi surface plays an increasingly important role as the hole doping p is increased. Thus, just as in $V_{2-x}O_3$ [23], large-moment antiferromagnetic insulator behaviour in the cuprates eventually gives way to small-moment incommensurate itinerant antiferromagnetic behavior as the system becomes more metallic [7,11]. Consistent with itinerant magnetism, the orbitally-averaged Fermi velocity $v_F = \sqrt{2e\hbar F}/m^* \approx 8 \times 10^4$ ms^{-1}, where F is the Shubnikov-de Haas oscillation frequency, of the pockets in $YBa_2Cu_3O_{6.5}$ [1,4] is comparable to the mode velocity $v_0 = 2aE_r/\pi\hbar\delta \approx 14 \times 10^4$ ms^{-1} (at $E = 0$) that one obtains fitting Eqn. 1 to the E-versus-$\mathbf{q}$ data points obtained from inelastic neutron scattering experiments on the same sample composition [14]. As p increases toward optimum doping, E_0 in Fig. 1(a) also increases [10,11,17], providing a suitable characteristic energy scale ($\sim$ 10s meV, *i.e.* $\sim$ 100s of Kelvin) for T_c [10].

The remaining ingredient in the problem is a coupling mechanism between the spin fluctuations and the charge inherent in the Cooper pair. This is found in the large onsite correlation energy U, which inhibits double occupancy of spins or holes [24]. Consequently, local variations in the density of holes $\Delta\rho_h$ and spin-density amplitude Δs are expected to be subject to the relation

$$\Delta\rho_h \propto -\Delta|s|. \qquad (5)$$

Pairing mechanisms involving this behavior have been considered both in the weak (small Hubbard U) [25] and strong (large Hubbard U) [26] coupling limits, although typically in conjunction with long-range antiferromagnetic order. However, there is no reason to suspect that such mechanisms will not apply in regimes where the antiferromagnetism is strongly fluctuating [11]. Therefore, because of the reciprocity relationship (Eq. 5), the slowly varying modulation of the spin fluctuation intensity should be accompanied by a concomitant charge modulation $\bar{\rho}_h(\mathbf{r}) \propto -|\bar{s}(\mathbf{r})|$. The very similar form of $\rho_h(\mathbf{r}) \propto -|s(\mathbf{r})|$ in the second column of Fig. 2 to $\rho_c \propto |\Psi(\mathbf{r})|^2$ in the third column of Fig. 2 therefore provides direct evidence for a 'spatial charge commensurability' between the Cooper pair wavefunction and incommensurate spin fluctuations.

In summary, based on measurements including Fermi-surface studies [1–5], neutron-scattering data [10–14] and resistivity experiments [20,21], we propose [16] that the unusually high superconducting transitions in the cuprates are driven by an exact mapping of the incommensurate spin fluctuations onto the $d_{x^2-y^2}$ Cooper-pair wavefunction. The spin fluctuations are driven by the Fermi-surface topology, which is prone to nesting [4,6,7]; they couple to the itinerant holes via the strong on-site Coulomb correlation energy U, which prohibits double occupancy of spins or holes [24]. The maximum energy of the fluctuations ($\sim$ 100s of Kelvin [10,11,17]) gives an appropriate energy scale for the superconducting T_c.

We are grateful to Neil Harrison, Suchitra Sebastian, Cyril Proust and Ed Yelland for stimulating discussions. This work is supported by the US Department of Energy (DoE) BES program "Science in 100 T". NHMFL is funded by the National Science Foundation, DoE and the State of Florida.

References

[1] N. Doiron-Leyraud *et al.*, Nature **447**, 565 (2007).
[2] E.A. Yelland *et al.*, Phys. Rev. Lett. **100**, 047003 (2008).
[3] A.F. Bangura *et al.*, Phys. Rev. Lett. **100**, 047004 (2008).
[4] S. E. Sebastian *et al.*, Nature, in press (2008).
[5] J. Singleton, P. Dai *et al.*, preprint (2008).
[6] S.R. Julian and M. Norman, Nature **447**, 537 (2007).
[7] N. Harrison *et al.*, Phys. Rev. Lett. **99**, 206406 (2007).
[8] R.D. McDonald *et al.*, preprint.
[9] C. Proust *et al.*, this conference.
[10] J.R. Schrieffer, and J.S. Brooks (Eds.), *High- temperature superconductivity theory and experiment* (Springer Science, 2007).
[11] A.P. Kampf, Phys. Rep. **249**, 219 (1994).
[12] K. Yamada *et al.*, Phys. Rev. B **57**, 6165 (1998).
[13] P. Dai *et al.*, Phys. Rev. B **63**, 054525 (2001)
[14] C. Stock *et al.*, Phys. Rev. B **71**, 024522 (2005).
[15] S. Wakimoto *et al.*, Phys. Rev. Lett. **92**, 217004 (2004).
[16] R.D. McDonald, N. Harrison and J. Singleton, preprint.
[17] P. Monthoux, A.V. Balatsky, and D. Pines, Phys. Rev. B **46**, 14830 (1992).
[18] C. C. Tsuei, and J. R.Kirtley, Rev. Mod. Phys. **72**, 696 (2000).
[19] A.M. Kadin, J. Supercon. Novel Magn. **20**, 285 (2007).
[20] Y. Ando, and K. Segawa, Phys. Rev. Lett. **88**, 167005 (2002).
[21] H.H. Wen *et al.*, Europhys. Lett. **64**, 790-796 (2003).
[22] G. Grüner, Rev. Mod. Phys. **66**, 1 (1994).
[23] W. Bao *et al.*, Phys. Rev. B **54**, R3726 (1996).
[24] F.C. Zhang, and T.M. Rice, Phys. Rev. B **37**, 3759 (1988).
[25] J.R. Schrieffer, X.-G. Wen, and S.-C. Zhang, Phys. Rev. Lett. **60**, 944-7 (1988).
[26] N. F. Mott, Phil. Mag. Lett. **64**, 211 (1991); A. S. Alexandrov. Physica C **305**, 46 (1998).
[27] J.M. Tranquada *et al.*, Nature **429**, 534 (2004); Phys. Rev. B **54**, 7489 (1996).